Article

Not peer-reviewed version

Design of Polylactic Acid Membranes for Controlled Release of Tramadol

Lafitte Fernández-Minotre , Mauricio Montero-Aguilar , Febe Carolina Vázquez-Vázquez , Janeth Serrano-Bello , Jose Vega-Baudrit , Reinaldo Pereira-Reyes , Amaury Pozos-Guillén , Daniel Chavarría-Bolaños *

Posted Date: 6 May 2025

doi: 10.20944/preprints202505.0085.v1

Keywords: scaffold; surgical membrane; tramadol; polylactic acid; air jet spinning; drug delivery system

 doi:10.20944/preprints202505.0085.v1

Article

Design of Polylactic Acid Membranes for Controlled Release of Tramadol

Lafitte Fernández-Minotre [1], Mauricio Montero-Aguilar [1], Febe Carolina Vázquez-Vázquez [2], Janeth Serrano-Bello [3], José Vega-Baudrit [4], Reinaldo Pereira-Reyes [4], Amaury Pozos-Guillén [5] and Daniel Chavarría-Bolaños [6,*]

[1] Dentistry Graduate Program, Universidad de Costa Rica, San José, Costa Rica
[2] Laboratorio de Materiales Dentales, DEPeI- Facultad de Odontología, UNAM, Ciudad Universitaria, Ciudad de México, Coyoacán, 04510, México
[3] Laboratorio de Bioingeniería de Tejidos, DEPeI- Facultad de Odontología, UNAM, Ciudad Universitaria, Ciudad de México, Coyoacán, 04510, México
[4] Laboratorio Nacional de Nanotecnología, Centro Nacional de Alta Tecnología, San José, Costa Rica
[5] Basic Science Laboratory, Facultad de Estomatología, Universidad Autónoma de San Luis Potosí, México
[6] Dentistry Graduate Program, Universidad de Costa Rica, San José, Costa Rica
* Correspondence: daniel.chavarria@ucr.ac.cr or danielchava2@gmail.com Tel.: +(506)2511-8054

Abstract: Background: This study aimed to develop polylactic acid (PLA)-based membranes incorporating tramadol (TMD) using air jet spinning (AJS), ensuring stable physicochemical properties and biocompatibility. Methods: Two groups were fabricated: 10% PLA membranes (control) and 10% PLA membranes loaded with TMD in an 80:1 ratio (experimental). Characterization included scanning electron microscopy (SEM), differential scanning calorimetry (DSC), thermogravimetric analysis (TGA), Fourier-transform infrared spectroscopy (FT-IR), ultraviolet-visible spectroscopy (UV-VIS), and biocompatibility assays with human osteoblasts using resazurin, crystal violet staining, and 5-chloromethylfluorescein diacetate for fluorescence microscopy. Results: SEM revealed a homogeneous, randomly distributed fiber pattern, with diameters under 5 µm and no structural voids. DSC and TGA indicated that TMD was uniformly incorporated, increased the thermal capacity, and slightly lowered the onset and inflection degradation temperatures. FT-IR confirmed the chemical compatibility of TMD with PLA, showing no structural alterations. UV-VIS detected sustained TMD release over 72 h. Biocompatibility tests showed no cytotoxic effects; cell viability and proliferation in TMD-loaded membranes were comparable to controls. Statistical analysis used ANOVA and Wilcoxon tests. Conclusions: 10% PLA membranes loaded with TMD at an 80:1 ratio exhibited stable physicochemical characteristics and favorable biocompatibility, supporting their potential use in drug delivery systems.

Keywords: scaffold; surgical membrane; tramadol; polylactic acid; air jet spinning; drug delivery system

1. Introduction

Postoperative pain is one of the main concerns dentists must deal with when per-forming surgical procedures like bone regeneration/augmentation. Pain is an unpleasant multidimensional sensation that varies in intensity, quality, duration, and reference. Pain is classified into several types: nociceptive, inflammatory, neuropathic, and functional [1]. Tissue engineering surgical procedures for bone regeneration unavoidably produce tissue damage, and due to local anesthesia, the nociceptive system ignores the injury and delays the body's defensive mechanism. This condition induces a systemic reaction through inflammatory pain aimed to heal the injured area by increasing sensitivity in the surgical site. The amplified sensitivity prevents further tissue damage during the postoperative period by minimizing movement or frictional contact of the healing site, such as a

 doi:10.20944/preprints202505.0085.v1

standard stimulus, which should usually not cause pain, but in the presence of a hypertensive area, the healing site will respond painfully. Therefore, clinicians must pharmacologically control the inflammatory pain without interfering with the healing process. Hence, the anti-inflammatory/analgesic treatment should aim to manage and not suppress the symptoms [2].

To achieve the above and strive for the patient's comfort, analgesics are prescribed systemically after the procedure. A long-time used drug with great potential and versatility is tramadol (TMD) due to its moderate analgesia capacity, synergy with anti-inflammatories, low possibility of causing allergic reactions, and efficacy in treating incisional pain. Some common side effects of TMD include nausea (6.1%), dizziness (4.6%), drowsiness (2.4%), fatigue (2.3%), sweating (1.9%), vomiting (1.7%), and dry mouth (1.6%). Although TMD has been demonstrated to be a broad-spectrum analgesic as a unimodal agent or combined with other analgesics, the side effects may contribute to clinicians' preference for different therapeutic approaches [3]. To reduce these unwanted effects, lower doses of TMD, used locally at the injury site, have been recommended. Local analgesia achieves a high local concentration of the drug with lower systemic levels, limiting adverse effects. In addition, pharmacological interactions are minimized and the use of the drug is facilitated without being limited depending on the tolerability dose [4]. Clinical positive results were obtained when TMD was placed into the tooth socket after third molar extractions, improving healing tolerance [5]. Studies have looked into the efficacy of combining TMD with local anesthetics such as lidocaine, mepivacaine, and articaine in local infiltration anesthesia procedures in the maxillae. In the case of lidocaine, it improved the anesthetic effect, healing, and perception of pain in patients [6,7]. The combination of TMD-mepivacaine showed encouraging results in the inferior alveolar nerve block, where the synergy between TMD-articaine for the surgery of impacted third molars and in the treatment of symptomatic irreversible pulpitis pain was clinically demonstrated [8].

Peripheral analgesia has been achieved through topical gels or creams, patches, aerosols, mouthwashes, and, the use of membranes for the controlled release of drugs locally [4]. Membranes are commonly used in dentistry for regenerative procedures, especially for guided bone regeneration. They are an essential element of tissue engineering based on its three main components: cells, their extracellular matrix (ECM), and a signaling system. Controlled manipulation of the extracellular microenvironment seeks to boost the ability of cells to organize, grow, differentiate, form an ECM, and, ultimately, develop new functional tissue [9]. The use of a membrane is fundamental, as it works as a barrier for soft tissues in guided bone regeneration processes and acts as a scaffolding to reconstruct soft tissues during the healing process of a wound. Membranes' desirable characteristics include biocompatibility, cell occlusion properties, integration capacity to host tissues, clinical manageability, space-creating ability, and suitable physico-mechanical properties. Resorbable membranes have been developed as a second generation of membranes that emerged to avoid the second surgical intervention that implied the removal of the non-resorbable membranes [10].

Resorbable membranes for bone regeneration have traditionally been synthesized with polymers using various manufacturing techniques. This polymer-based material provides porous and three-dimensional membranes, striving to create a biomatrix framework with resemblant geometric characteristics to the ECM, in which a cell interacts with its substrate [11,12]. Biodegradable polymers used to manufacture membranes are further classified as natural or synthetic. Polylactic acid (PLA) is highly relevant as a synthetic polymer with great potential in biomedical applications [9]. Among PLA's various qualities, we can mention its workability, processability, biodegradation, low cost, and drug encapsulation capacity [11,13-17].

Some of the most traditional methods for manufacturing polymeric membranes and scaffolds are electrospinning and air jet spinning (AJS). The AJS technique can be considered the most advantageous from the point of view of industrialization and scalability because it's faster and easier to use, it's less expensive than other techniques, safe because it does not use high voltage in the processing, and its versatility in the choice of solvent. AJS uses pressurized gas dispensed at extreme speed to stretch the polymer solution into thin fibers, which, as mentioned, are deposited on a substrate, producing micro and nanoscale fibers of different polymers [10,17,18].

 doi:10.20944/preprints202505.0085.v1

Polymer therapy is a growing and important area of biopharmaceuticals that seeks to use linear or branched polymer chains as a bioactive element to which a therapeutic agent (usually a drug) is covalently bound. This binding improves its pharmacokinetic and pharmacodynamic properties such as an increased plasma half-life (less frequent dosing is required), resistance to proteolytic enzymes, reduced immunogenicity, better protein stability, better low drug solubility, low molecular weight, and the potential for locally directed action [17-20]. The development of more efficient, biocompatible, biodegradable barriers and scaffolds that can be used for tissue engineering and could also provide a slow controlled drug delivery system, releasing an analgesic drug locally to provide lasting comfort for patients undergoing a regeneration treatment, is still an undergoing process. Hence, the objective of this study was to produce TMD-loaded PLA nanofibers to manufacture resorbable membranes using the AJS technique with stable and biocompatible physicochemical characteristics.

2. Results

2.1. Macro and Microphotograph Analysis:

It was possible to synthesize 10% PLA membranes loaded with tramadol in an 80:1 polymer-drug ratio. Macroscopically, these membranes have a soft texture and white-transparent color. Although they can be isolated, separated, and cut, their handling is delicate to avoid distortion of the biomaterial. At 40X magnification of the light microscope, it is possible to appreciate a random arrangement of the PLA fibers for both groups with areas of different membrane densities. When analyzed by SEM at lower magnification (50X), it was difficult to detect differences between the groups. The membranes showed a random distribution of polymer fibrils with no voids or empty areas. At 2,000X and 5,000X magnifications, it was possible to observe longitudinal fibers oriented in different planes and angulations (Figure 1). The average fiber size was 0,79um (± 0,11) um and 0,68 (± 0,12) for control and Tramadol charged membranes respectively, showing no statistical differences between them ($p > 0,05$) (Figure 2). In some areas, it is possible to see the formation of plates or larger constructs by the precipitation of individual fibers

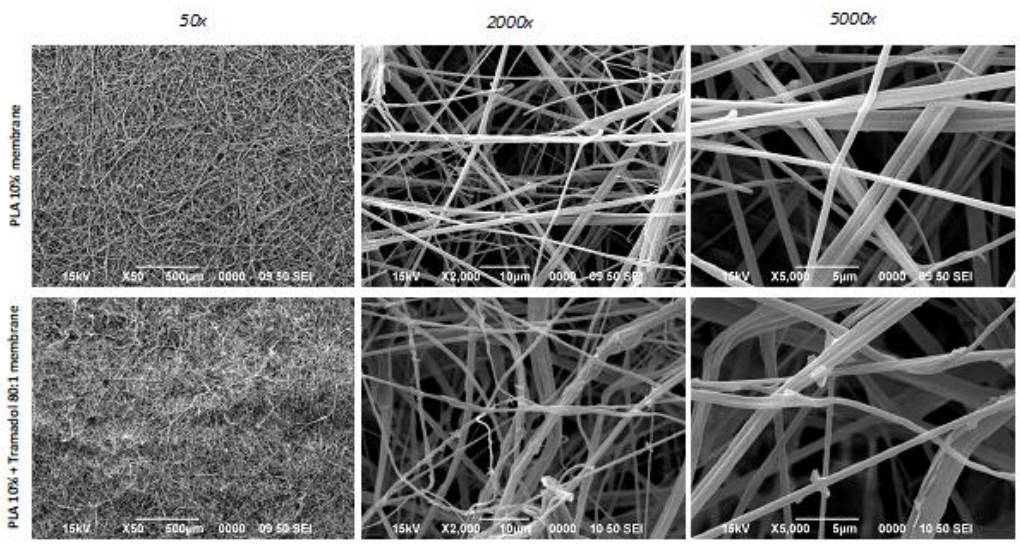

Figure 1. SEM analysis at 50X, 2,000X, and 5,000X magnifications show control and experimental membranes with a random disposition of the fibers.

 doi:10.20944/preprints202505.0085.v1

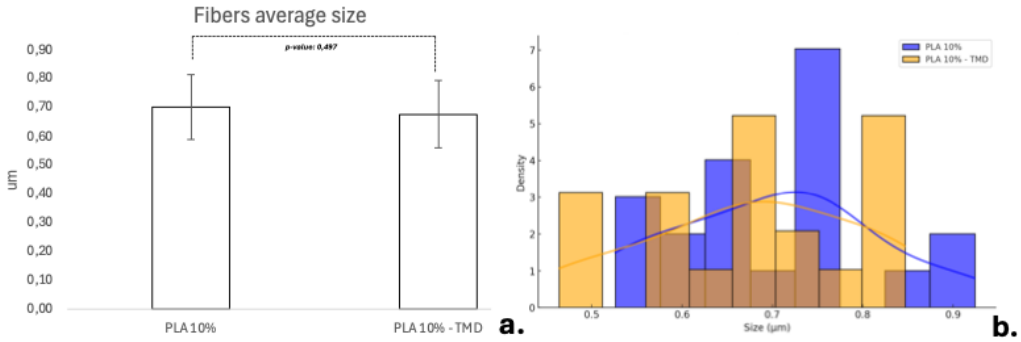

Figure 2. a. Average size of individual fibers for each group. **b.** Histogram with density curves (fibers size distribution).

2.2. Analysis of Thermodynamic Profile

2.2.1. Differential Scanning Calorimetry (DSC):

It was observed that the control group presented different calorimetric curves than the pure polymer (PLA pellet), which didn't show the first endothermic signal and showed a well-defined second signal (Figure 3). When analyzing the calorimetry of the experimental group, it was evident that it didn´t display the endothermic peak of pure TMD, indicating that the drug was homogeneously and stably incorporated into the system. Subsequently, DSC analysis was conducted five times for both the control and experimental groups to verify the purity of the samples. Figure 4 shows that the maximum temperature and heat capacity of the first signal showed no statistical differences ($p > 0.05$). The only statistically significant difference was the heat capacity observable in the TMD-loaded membrane ($p < 0.05$), indicating that the presence of the drug increases the heat capacity of the polymeric system (Figure 5).

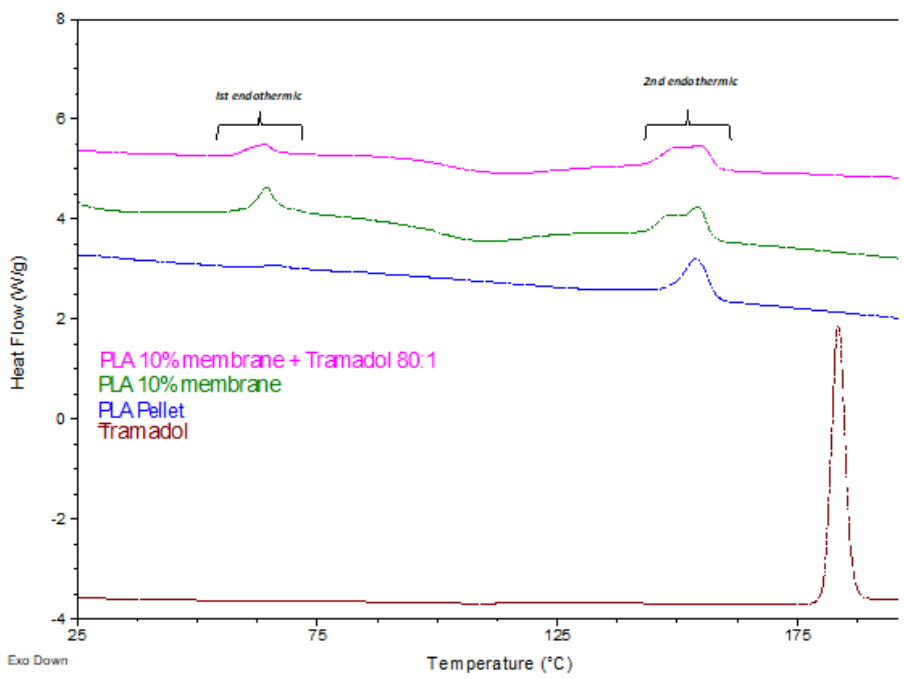

Figure 3. DSC thermograms of neat PLA, 10% PLA membrane, pure TMD, and 10% PLA+TMD membrane.

 doi:10.20944/preprints202505.0085.v1

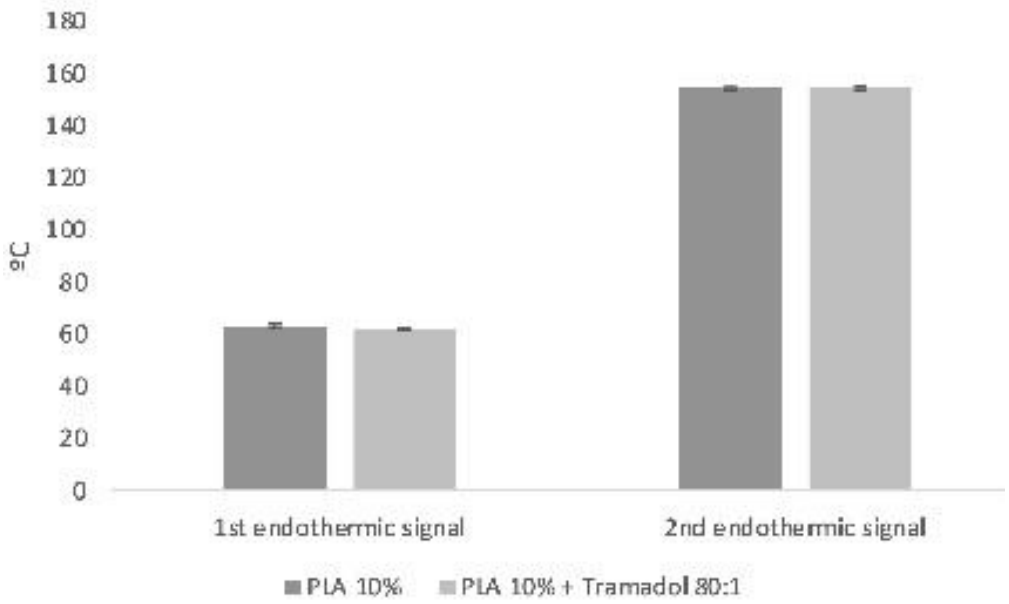

Figure 4. Maximum temperature (°C) of the first and second signal of endothermic capacity for experimental and control groups.

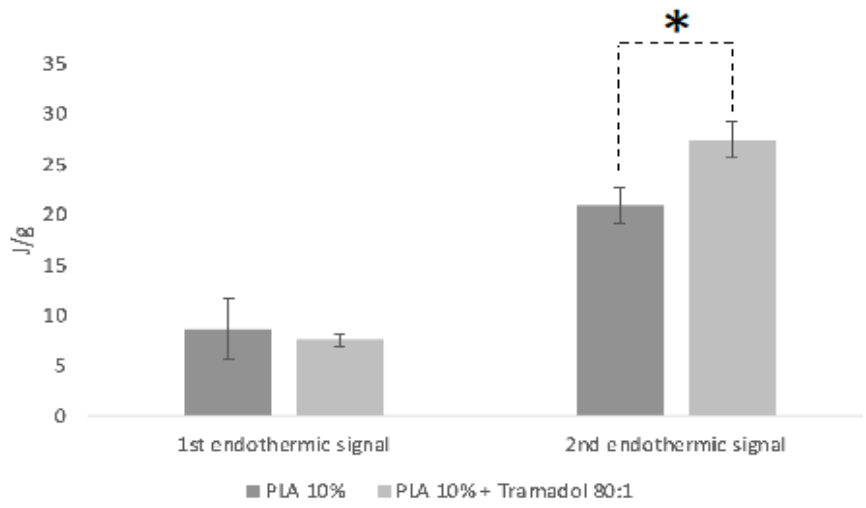

Figure 5. Heat capacity (J/g) of the first and second signal of endotermic capacity for the experimental and control groups.

2.2.2. Thermogravimetric Analysis (TGA):

TGA analysis showed the absence of impurities or by-products during the membrane manufacturing process. The 10% PLA membranes and the 10% PLA + TMD membranes showed a single mass drop, with a visible OnSet Point (To), as well as a single point of inflection (Tp) (Table 1), calculated by the derivative of the weight percent change/temperature. (Figures 6) Pure tramadol also showed a single mass drop curve, with visible To and Tp (Table 1).

 doi:10.20944/preprints202505.0085.v1

Table 1. Values of thermogravimetric parameters. TMD decreases the To and Tp of the PLA 10% membranes.

Product	Onset point (To) (ºC)	Inflection points (Tp) (ºC)
Tramadol	234,39	270,57
PLA 10% membrane	310,24	343,35
PLA 10% membrane + Tramadol 80:1	302,33	334,40

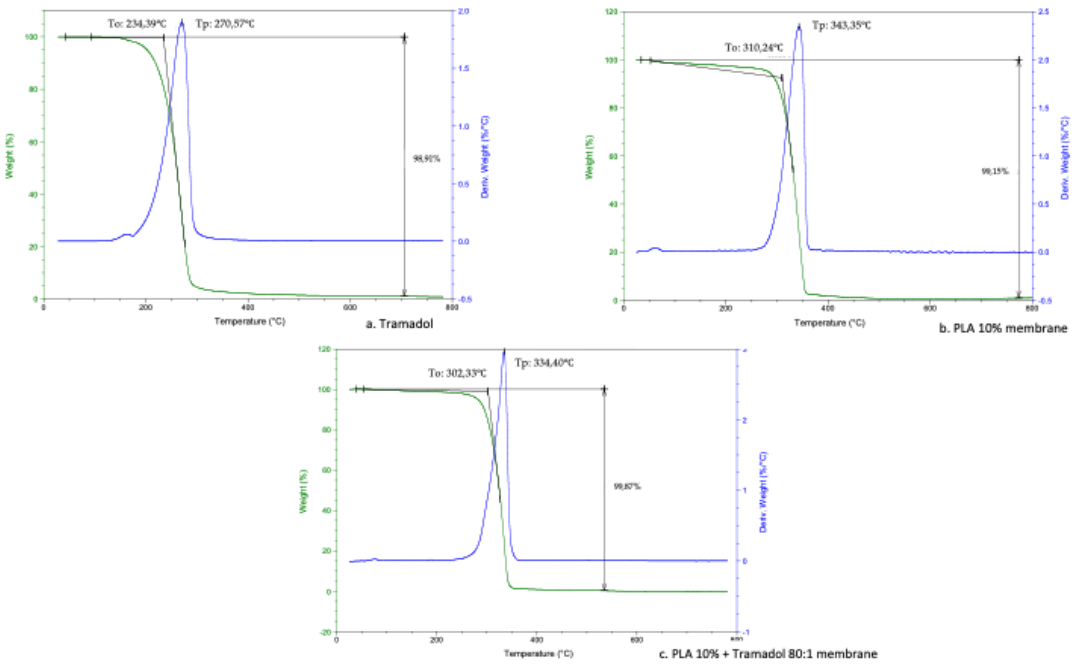

Figure 6. TGA analysis showing onset points (To), inflection point (Tp) and maximun weight loss percentage at 800ºC. a. Pure Tramadol. b. PLA 10% membrane. c. PLA 10% + Tramadol 80:1 membrane.

2.3. Chemical Composition

2.3.1. FT-IR Analysis:

FT-IR results demonstrated that manipulating the polymer to synthesize the membranes does not alter their composition. Similarly, adding TMD was compatible with the polymer and did not alter the infrared profile. Changes in the signals at 2900, 1650 and 1500 cm-1 were observed in the charged membranes, not in the control ones; which were attributable to the presence of tramadol. At a higher magnification, it was identifiable an symmetric CH2 signal measurable between 2900 and 2800 cm-1, and the asymmetric signal of 2933 cm-1 of the methylene group, previously described for this molecule. The other tramadol signals may have gone unnoticed due to the low proportion of the drug and its incorporation into the polymer matrix before AJS synthesis (Figure 7).

 doi:10.20944/preprints202505.0085.v1

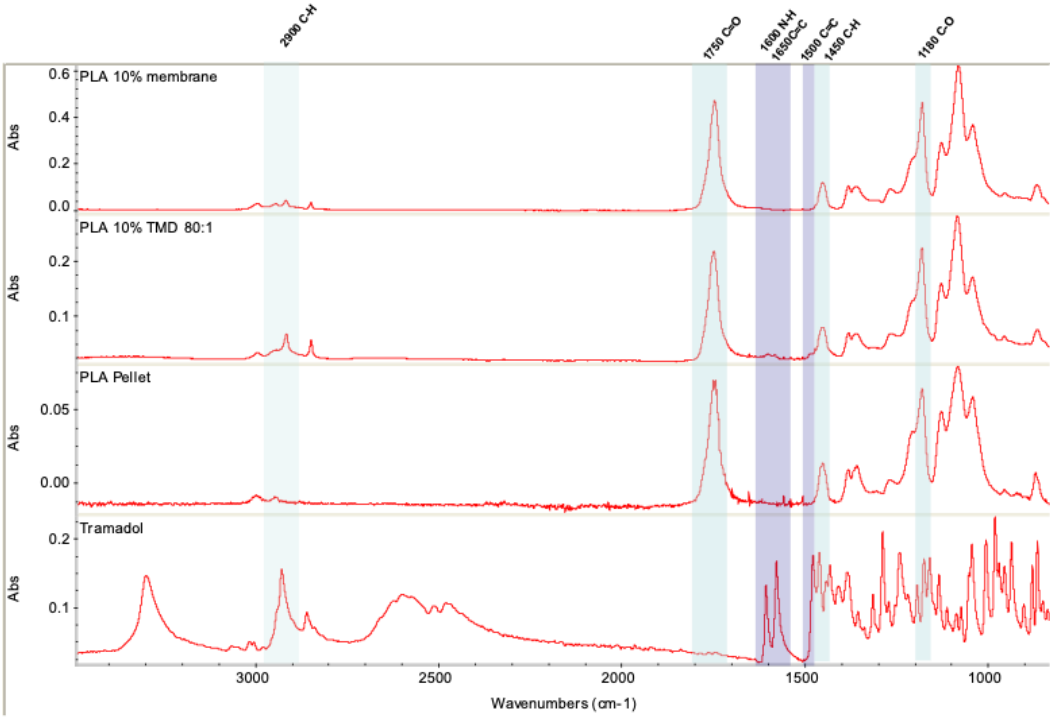

Figure 7. The chemical structure of TMD, pure PLA, PLA 10% membrane, and PLA 10% + TMD membrane were analyzed by FTIR within the range of 400-4000 cm-1.

2.3.2. UV-VIS Spectrometric Analysis

It was possible to identify the presence of tramadol in the recovered aliquots, specifically 185,31 ±2,1 µG/mL, 180,80±15,27 µG/mL y 174,88±16 µG/mL for 24, 48, and 72 hours respectively. This finding demonstrates that TMD was indeed loaded on the membranes and could be recovered by hydrolysis of the system (Figure 8). None of the alliquotes recovered from the control membranes showed any presence of tramadol, neither absorption changes at this specific wavelength.

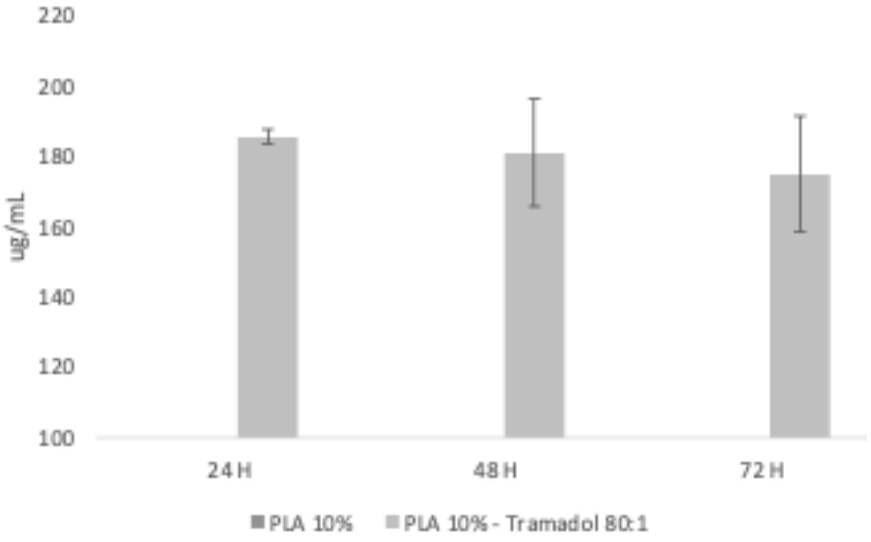

Figure 8. TMD concentration per aliquot at different times.

 doi:10.20944/preprints202505.0085.v1

2.4. Biocompatibility Analysis

The biocompatibility of PLA fibers spun mat and PLA loaded with tramadol was analyzed at in vitro cell culture to investigate the cell viability of hFOB 1.19 cells. The results are presented as the optical absorbance of 545 nm. The histogram in Figure 9 suggests that in the scaffolds the presence of tramadol didn´t showed any adverse effects on cell viability and there were no significant differences in comparison with the control PLA witouth loaded TMD.

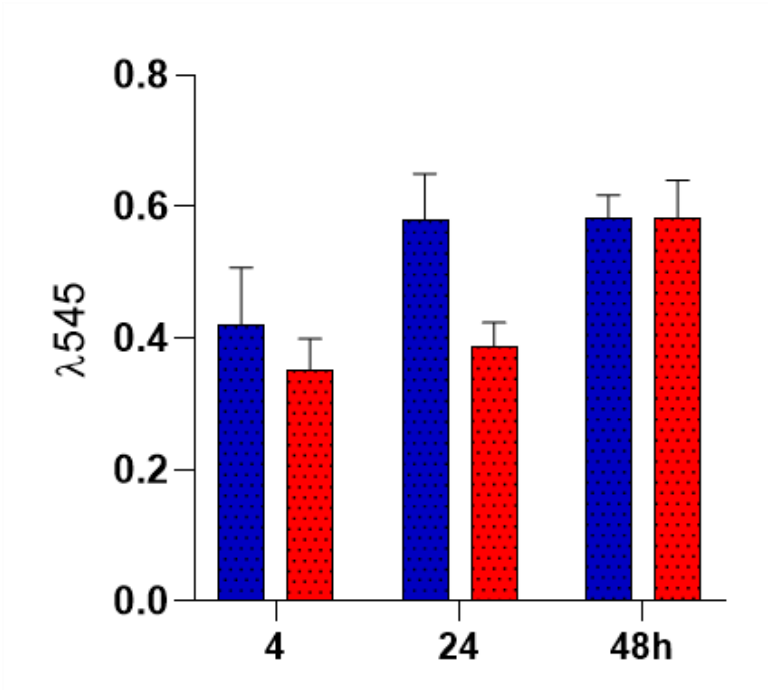

Figure 9. Cell viability response of hFOB after 4, 24 and 48 h cultured onto PLA spun mat loaded with tramadol 80:1 ( ) and control 10 % PLA spun mat ( ).

2.4.1. Colonization of PLA Spun Membrane

The colonization over the surface of the PLA fiber spun mat showed that the presence of tramadol do not affect the interaction of the cells in the topographical fiber cues of the polymeric material. This behaviour is in agreement with the viability test and the green CFMDA also showed that hFOB cells are viable and spreading in the surface of the PLA membrane after 48 h in both control (Figue 10 A) and experimental group (Figure 10 C). In addition, the homogeneous distribution of the cells covering the fiber topography of the PLA membranes was observed by SEM micropgraphs and also it could be apreciated the interaction with the neighboring cells and follow the random orientation of the fibers (Figure 10 B and D).

 doi:10.20944/preprints202505.0085.v1

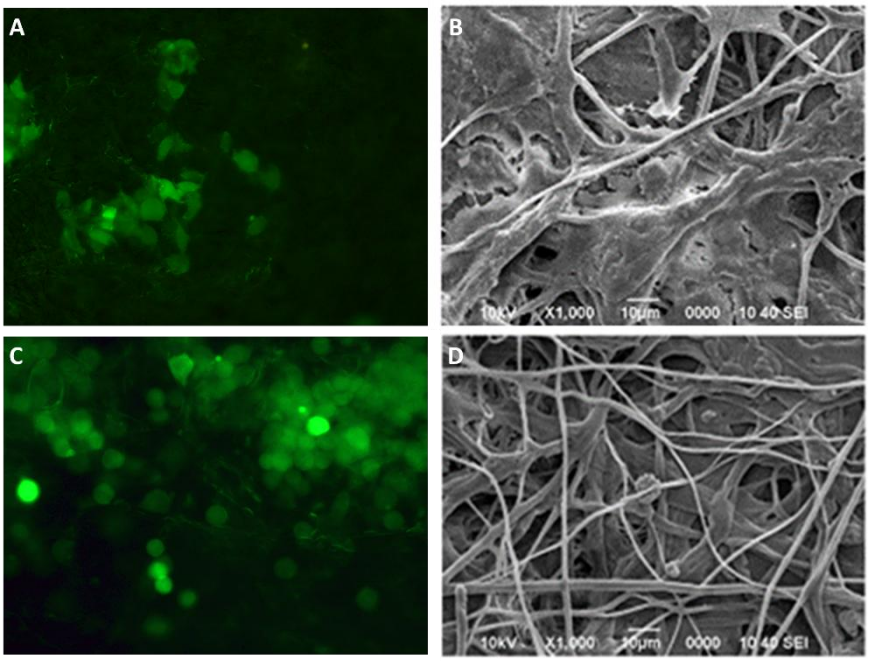

Figure 10. Colonization and spreading patter of hFOB cultured onto PLA fibers spun mat (A and B) and PLA loaded with tramadol (C and D) after 48 h.

3. Discussion

The AJS technique was chosen mainly due to the feasibility to customize and synthetize PLA nanofibrillar membranes to be used as a drug delivery system. This technique offers important advantages such as low-cost synthesis equipment, fabrication speed and non-voltage source needed [18,21]. In our research, the AJS method allowed a predictable way to obtain 10% PLA membranes with and without TMD at a concentration of 80 : 1. As indicated by Medeiros et al. who compared the efficiency of the AJS and electrospinning methods; AJS method allows to obtain a range of micro and nanofibers from different polymer solutions in the same size range as fibers made by electrospinning but with greater potential for commercial scale-up; offering also the possibility to coat different kinds of materials including those sensible to thermal changes or voltage sensitive polymers. To assure a proper result from AJS method, there must be an optimal relationship between gas flow pressure, solution feed rate and working distance for the solvent to evaporate and form solidified naonfibers on the receptor [22]. Previous study analyzed the correlations between solution-blown, fiber morphology and annular turbulent airflow fields under different air pressures, that straight segment length of the polymer solution jet, velocity fluctuations, flapping motion and solvent evaporation affect the final fiber morphology, with more uniform and smaller diameters when air pressure was increased; however, more uneven fibers are obtained and the appearance of some fiber strands [23].

Stojanovska et al, developed a list of parameters to be considered during the processing of membranes and scaffolds by AJS, where they highlighted the polymer concentration, air pressure, diameter of the ejector nozzle, and synthesis distance as the main aspects to control [17]. In the present investigation, an air pressure of 30 psi, a 0.3 mm exit nozzle pointed to a receptor frame located at a distance of 11 cm and a PLA concentration of 10% PLA was selected, based on the methodology used by Suarez-Franco et al, who studied the influence of PLA concentration at 6%, 7% and 10% on membrane biocompatibility, concluding that cell adhesion and proliferation was improved with the highest concentration [11]. Although lower concentrations were also considered, preliminary pilot data showed that the formation of nanofibers was also enhanced at this concentration once the drug was added. With respect to the concentration of the drug, previous tests performed determined that the 80:1 concentration was the most favorable in terms of fiber stability

 doi:10.20944/preprints202505.0085.v1

and drug stability. By combining the PLA concentration and drug charge, it was possible to obtain membranes with similar microtopographic characteristics, showing random distribution of polymer nanofibers oriented in various planes and angulations, with a fiber size not exceeding a 5 μm diameter. PLA is an excellent biomaterial to achieve characteristics such as those achieved in the present study and that favor the qualities as a scaffold for tissue regeneration, but its use in bone regeneration procedures has been debated because of its mechanical qualities, however, criticisms are made when the membranes have been fabricated by electrospinning and not AJS, being the AJS technique the one that most favors random deposition, fiber morphology, pore formation and polymeric solution behavior to achieve better physico-mechanical qualities; However, in the present study, a difficult handling of the samples was noted, so future studies should focus on improving this aspect, as cited by Bharadwaz et al, who indicate that to improve the mechanical strength of PLA scaffolds, it has been opted to make mixtures with other polymeric fibers or modify the structure of the polymer as such [24,25,26].

Thermodynamic analyses obtained by DSC and TGD allowed to analyze the effect of the components added to a polymeric matrix and its homogeneity and stability, as well as the presence of impurities or contaminants from the manufacturing process. DSC demonstrate the absence of the characteristic endothermic peak of TMD, which is identifiable at approximately 180°C. Such absence could be due to the loss of the crystalline structure of the drug once dissolved and mixed with the polymer [27]. In addition, a change in the thermal capacity of the charged membrane was identified, for which it is assumed that the drug was homogeneously and stably incorporated in the system. A similar finding was reported by Kumar et.al. when samples of an alginate- gelatin gel loaded with TMD was analyzed by DSC. They noticed the absence of the drug endothermic signal, indicating that it is a product of a possible shielding of the TMD by a drug-polymer inclusion complex [28]. Present results showed a remarkable change in the thermodynamic profile of the membranes charged with TMD. As previously reported, a change in the mass of the materials implies a chemical change that is reflected in the thermodynamic characteristics [29,30]. In the TGA the presence of TMD, decreases the To and Tp of the PLA 10% membrane, behavior similar to the study of Maubrouk et al, where the effect of TMD in poly(Ɛ-caprolactone) tapes was assessed [31]; in addition, the TGA demonstrated the efficiency of the method of handling and production of the samples by not identifying process impurities.

The incorporation of TMD into the 10% PLA membrane was evaluated by Fourier transform infrared spectrometry (FT-IR). The results show that the manipulation of the polymer for the synthesis of the membranes does not alter its composition. Similarly, the incorporation of TMD is compatible with the polymeric system, and does not affect the infrared profile, which is in agreement with previous studies that incorporated the drug into a polymeric matrix [28,29,32-34]. In order to verify that the TMD was loaded on the membranes and that it can be release from the matrix, UV-VIS analysis was used. According to Küçük and Kadıoğlu, it is possible to determine the presence of TMD in methanol and water by means of an ultra violet spectrophotometer at a reading wavelength of 271 nm [35], while PLA is measurable at approximately 230nm. The controlled release assay performed to the membranes demonstrated that it was possible to recover TMD form the water aliquots, identifying the presence of TMD at 24, 48 and 72 h. Future studies will be designed to analyze the relationship between theoretical and recovered loading; as well as the release kinetics as a function of time. A limitation of the present study was that recovery aliquots were obtained using only distilled water grade 3, with a pH between 5.0 and 7.5 at 25°C according to the ISO 3696 Standard [36]. Therefore, future studies should evaluate the behavior of the membrane with the drug in other media such as different pH levels, or biological fluids such as saliva or blood [29].

To determine the biocompatibility of the samples, the cytotoxicity of 10% PLA membranes and 10% PLA membranes with TMD was evaluated by means of staining tests to quantify cell adhesion and proliferation. As it was previously reported, the cellular behavior is influenced by the environment, so customized scaffolds must try to resemble the microarchitecture of the ECM. Therefore, polymeric matrices must provide an environment that allows these dynamic behaviors of

 doi:10.20944/preprints202505.0085.v1

cells through nanopores and fibers morphologically compatible with the minimum mechanical requirements [11,37,38]. The biocompatibility of PLA scaffolds is widely accepted. Granados-Hernandez et al. evaluated the response of human bone marrow mesenchymal stromal cells in 10% PLA scaffolds obtained by AJS, showing that after different culture periods cytotoxicity was absent [21]. In the present study, the use of a line of human fetal osteoblasts and the crystal violet staining assay, allows confirming the biocompatibility of the unloaded scaffolds, and the possible biological changes under the presence of TMD, since, the staining detects only living cells due to the fact that the dye binds to the chromatin and nucleus of them. The membrane results obtained were consistent with previous reports that have used a methodology similar to the one presented here, confirming that the designed scaffolds are suitable for enhancing cell proliferation [39,40]. The results also showed an increased growth in the charged scaffold, which was slightly decreased but not inhibited by the presence of TMD. These results confirmed that charged membranes didn´t generate an immediate cytotoxic response.

Cell adhesion on the surface of the membranes was also evaluated, showing no difference between groups at 24 and 48 h. To determine this, the rezasurin staining test was used to evaluate cell adhesion due to its non-toxic permeability to the cells. It also offers important information about cell vitality, since its reduction to resofurin depends of mitochondrial activity [41]. TMD-loaded membranes shown a biocompatible behavior since cell adhesion was maintained during observation periods, and was comparable to control membranes. The cell-membranes interaction was evaluated by fluorescence microscopy and scanning electron microscopy. Fluorescence microscopy allows to evaluate not only cell viability on the membranes, but also their distribution and morphology. Because the CellTracker™ has an affinity for lipids, the stain will only emit its signal upon binding to the intact cell membrane. In the microphotographs, cell presence and viability were observed at 48 h post culture and was comparable between both groups. In addition, we can identify the position and homogeneous distribution of the cells on the membranes, the hexagonal morphology characteristic of osteoblasts, and it was possible to identify cytoplasmic prolongations to start interacting with neighboring cells by means of their lamellipodia, all of which indicates that charged membranes with TMD 80:1 didn´t affect cellular response. Scanning electron microscopy also showed some of the behavior observed by fluorescence, confirming in tridimensional images the cell morphology and surface integrity. These findings support that these nanofibrillar membranes offers promising biological properties to enhance cellular response [18,38,39]. A key aspect to achieve biocompatibility was the low dosage of TMD present in the membranes, and the avoidance of chemical toxins after the membrane's synthesis. According to dos Santos, in his study on hydrogels for TMD administration, the higher the concentrations of the drug, the higher the in-vitro cytotoxic potential and this harmful effect could be attenuated by the medium used to transport the drug [42]. Therefore, the PLA could be counteracting the cytotoxicity of the drug and this could explain the reason why the experimental group did not have such a large increase in cell proliferation as the control group, but ultimately it did increase but slightly. Future research should analyze whether the dose of TMD in the membranes is sufficient to achieve the desirable clinical effects.

4. Materials and Methods

4.1. Polymer Fiber Fabrication of PLA Loaded with Tramadol

Fibrous spun scaffolds were fabricated via the air jet spinning process from PLA polymeric solutions of 10 % wt. First, polymeric solutions of 10 % wt of PLA were prepared: PLA pellets ($C_3H_6O_3$; molecular weight (MW) 192,000, designated Ingeo Biopolymer 2003D from Promaplast, Mexico) were dissolved in chloroform (CHCl3) and stirred for 20 hours. After that, anhydrous absolute ethyl alcohol (CH_3CH_2OH, J. T. Baker) was added, and let the solution stirring for 30 minutes up to obtain a homogeneous solution. The volume ratio of chloroform/ethanol was 3:1. Then, the polymeric solution was prepared with tramadol (Tramadol HCL, code 15101782, lot 3735ID12) to obtain a mixture with a volumetric ratio of 80:1 for the composite fiber scaffold. The synthesis of the

 doi:10.20944/preprints202505.0085.v1

membranes, in all cases, the polymeric solution was placed in a commercially available airbrush ADIR model 699 with a 0.3 mm nozzle diameter and with a gravitational feed of the solution to synthesize the fiber membrane scaffolds. The airbrush was connected to a pressurized argon tank (CAS number 7740-37, concentration > 99%, PRAXAIR Mexico). For deposition of the fibers, a pressure of 30 psi with 11 cm of distance from the nozzle to the target was held constant. Once the fibers were obtained, they were subjected to analysis of their physicochemical and structural properties.

4.2. PLA Loaded with Tramadol Fiber Scaffold Characterization

The morphology and structure of the fibers were observed with a scanning electron microscope (SEM, JSM 7600F, JEOL, USA). Chemical structure of fibers was analyzed by Fourier transform infrared spectrophotometer (FTIR) employing the Nicolet iS50 (ThermoFisher, Madison, USA) spectrometer within the 400–4,000 cm−1 range.

Thermogravimetric analysis (TGA) was done using TGA-Q500 equipment (TA In-struments, Delaware, USA). Platinum baskets were tared before automatically weighing 4-6 mg of the sample to be analyzed. After loading, the furnace was closed and running on a ramp from 25 °C to 800 °C, with a heating rate of 10 °C/min. Data were analyzed using TGA software (Universal V4.5A TA Instruments) to identify onset points (To), inflection points (Tp), and maximum mass loss point (Tmax).

Differential scanning calorimetry (DSC) (Q200, TA Instruments, Delaware, USA) was performed with 2 mg of each sample, running a ramp from 25 °C to 250 °C, with a heating rate of 10 °C/min. Glass transition temperature (Tg) and melting points (Tm) were calculated.

UV-Vis spectroscopy was used to confirm the presence of TMD in the synthesized membranes and the release from the spun scaffold. The equipment was first calibrated using a TMD curve (271 nm wavelength). Then, membrane specimens weighing 23 mg of the experimental group were placed in a Transwell system with 12 mm diameter inserts and polycarbonate membranes with 0.4µm pores. Each well was filled with 1.5 mL of distilled water and incubated at 37°C and after 24, 48, and 72 h, after the time 1 mL aliquot was retrieved for spectroscopy analysis. The experiment was performed in triplicate.

4.3. In Vitro Studies

Human fetal osteoblast cells (hFOB, 1.19 ATCC CRL-11372) was used to evaluate the cell biocompatibility response of PLA fibers spun mat and PLA loaded with tramadol. hFOB cells were cultured in 75 cm^2 cell culture flasks containing a 1:1 mixture of Ham´s F12 medium Dulbecco's Modified Eagle Media (DMEM, Sigma-Aldrich, St. Louis, USA), supple-mented with 10% fetal bovine serum (FBS, Biosciences, USA), 2.5 mM L-glutamine and antibiotic solution (streptomycin 100 µg/mL and penicillin 100U/mL, Sigma-Aldrich). The cell cultures were incubated in a 100% humidified environment at 37°C in 95% air and 5% CO_2. hFOB on passages 2-6 were used for all the experimental procedures. Before the biological assays, PLA fibers spun mat and PLA loaded with tramadol were sterilized by UV light for 10 min. To evaluate the cell viability of the hFOB onto fiber scaffold, cells were seeded at $1x10^4$ cells/mL and analyzed after 24, 48, and 72 h of culture. The viability was checked by the resazurin colorimetric assay after prescribed time 20 µl of resazurin solution (BioReagent R7017, CAS number 62758-13-8) was added to the samples and incubated for 4 h at 37°C. Then, 200 µL of the supernatant was removed, and absorbance was quantified by spectrophotometry at 545 nm with a ChroMate plate reader (Awareness Technology, MN, USA).

Colonization and spreading interaction of hFOB cells seeded at 1 x 10^4 cells/mL onto PLA fibers spun mat and PLA loaded with tramadol were examined after 48 h using SEM and epifluorescence microscopy. For fluorescence observation, before seeding the hFOB 1.19 cells onto the fiber membrane scaffold, cells were incubated with CellTracker™ Green (CMFDA, 5-chloromethylfluorescein diacetate) in phenol red-free medium at 37°C for 30 min. Subsequently, the cells were washed with PBS and incubated for 1 h in a complete medium. Then, hFOB 1.19 cells were

 doi:10.20944/preprints202505.0085.v1

trypsinized and counted to the desired cell concentration (1 x 10^4 cells/mL) incubated for 48 h and examined under the epifluorescence inverted microscopy (AE31E, MOTIC). For SEM analysis, after 48 h of incubation, scaffolds were washed three times with PBS, fixed with 2% glutaraldehyde, then dehydrated with a graded series of ethanol (25-100%) and air-dried. Next, the samples were sputter-coated with a thin layer of gold and examined by SEM.

4.4. Statistic Analysis:

Fiber's diameter was analyzed, and average data was compared by T-test. For the biocompatibility tests, the statistics were performed using Analysis of Variance (ANOVA) and the Wilcoxon test for the DSC data analysis.

Author Contributions: For research articles with several authors, a short paragraph specifying their individual contributions must be provided. The following statements should be used "Conceptualization, L. F.-M., F. V.-V., A. P.-G., and D. Ch.-B.; methodology, L. F.-M., M. M.-A., J. S.-B., R. P.-R., and D. Ch.-B.; software, M. M.-A., J. S.-B., and J. B.-V.; validation, M. M.-A., F. V.-V., R. P.-R. and D. Ch.-B.; formal analysis, M. M.-A., A. P.-G., and D. Ch.-B.; investigation, L. F.-M., F. V.-V., R. P.-R.; resources, J. B.-V. R. P.-R., F. V.-V., and D. Ch.-B.; data curation, L. F.-M., F. V.-V., and R. P.-R.; writing—original draft preparation, L. F.-M., F. V.-V., and D. Ch.-B.; writing—review and editing, M. M.-A., F. V.-V., J. S.-B., R. P.-R., A. P.-G., and D. Ch.-B.; visualization, M. M.-A., J. S.-B., R. P.-R., and D. Ch.-B.; supervision, A. P.-G., and D. Ch.-B.; project administration, D. Ch.-B.; funding acquisition, J. B.-V., and D. Ch.-B. All authors have read and agreed to the published version of the manuscript.

Funding: This research received no external funding.

Acknowledgments: The authors thank the Universidad Nacional Autónoma de México, Universidad de Costa Rica and

Conflicts of Interest: The authors declare no conflicts of interest.

Abbreviations

The following abbreviations are used in this manuscript:

PLA	Polylactic acid
TMD	Tramadol
AJS	Air jet spinning
SEM	Scanning electron microscopy
DSC	Differential scanning calorimetry
TGA	Thermogravimetric analysis
ANOVA	Analysis of variance
ECM	Extracellular matrix
MW	Molecular weight

References

1. Woolf, C. J. Pain: moving from symptom control toward mechanism-specific pharmacologic management. *Ann. Intern. Med.* **2004**, 140 (6), 441–451.
2. Barakat, A. Revisiting tramadol: A multi-modal agent for pain management. *CNS Drugs* **2019**, 33(5), 481–501.
3. Sawynok, J. Topical and peripherally acting analgesics. *Pharmacol. Rev.* **2003**, 55(1), 1–20.
4. Pozos-Guillén A.J.; Aguirre-Bañuelos, P.; Arellano-Guerrero, A; Castañeda-Hernández, G.; Hoyo-Vadillo, C.; Pérez-Urizar, J. Isobolographic analysis of the dual-site synergism in the antinociceptive response of tramadol in the formalin test in rats. *Life Sci.* **2006**, 79(24), 2275–2282.
5. Ege, B.; Ege, M.; Koparal, M.; Alan, H. Comparison of the anesthetic efficiency of lidocaine and tramadol hydrochloride in orthodontic extractions: a split-mouth, prospective, randomized, double-blind study. *J. Oral Maxillofac. Surg.* **2020**, 78(1), 52–62.

 doi:10.20944/preprints202505.0085.v1

6. Bolaños, D. C.; Guillén, A. P. Peripheral tramadol in dentistry: A new use for an old drug. *Odovtos-Int. J. Dent. Sc.* **2016**, 18(2), 10–14.
7. Scheller, E. L.; Krebsbach, P. H.; Kohn, D. H. Tissue engineering: state of the art in oral rehabilitation. *J. Oral Rehabil.* **2009**, 36(5), 368–389.
8. Elgali, I.; Omar, O.; Dahlin, C.; Thomsen, P. Guided bone regeneration: materials and biological mechanisms revisited. *Eur. J. Oral Sci.* **2017**, 125(5), 315–337.
9. Bottino, M. C.; Thomas, V. Membranes for periodontal regeneration-A materials perspective. *Front. Oral Biol.* **2015**, 17, 90–100.
10. Suarez-Franco, J. L.; Vázquez-Vázquez, F. C.; Pozos-Guillen, A.; Montesinos, J. J.; Alvarez-Fregoso, O.; Alvarez-Perez, M. A. Influence of diameter of fiber membrane scaffolds on the biocompatibility of hPDL mesenchymal stromal cells. Dent. Mater. J. **2018**, 37(3), 465–473.
11. Lu, Y.; Aimetti, A. A.; Langer, R.; Gu, Z. Bioresponsive materials. *Nat. Rev. Mater***. 2016**, 2(1), 1–17.
12. Schenk, R. K.; Buser, D.; Hardwick, W. R.; Dahlin, C. Healing pattern of bone regeneration in membrane-protected defects: a histologic study in the canine mandible. *Int. J. Oral Maxillofac. Implants* **1994**, 9(1), 13–29.
13. Garlotta, D. A literature review of poly (lactic acid). *J. Polym. Environ.* **2001**, 9(2), 63–84.
14. Saini, P.; Arora, M.; Kumar, M. R. Poly (lactic acid) blends in biomedical applications. *Adv. Drug Deliv. Rev.* **2016**, 107, 47–59.
15. Murariu, M.; Dubois, P. PLA composites: From production to properties. *Adv. Drug Deliv. Rev.* **2016**, 107, 17–46.
16. Stojanovska, E.; Canbay, E.; Pampal, E. S.; Calisir, M. D.; Agma, O.; Polat, Y.; Kilic, A. A review on non-electro nanofibre spinning techniques. *RSC Adv.* **2016**, 6(87), 83783-83801.
17. Abdal-hay, A.; Sheikh, F. A.; Lim, J. K. Air jet spinning of hydroxyapatite/poly (lactic acid) hybrid nanocomposite membrane mats for bone tissue engineering. *Colloids Surf. B Biointerfaces* **2013**, 102, 635–643.
18. Tseng, Y. Y.; Liu, S. J. Nanofibers used for the delivery of analgesics. *Nanomedicine* **2015**, 10(11), 1785–1800.
19. Liechty, W. B.; Kryscio, D. R.; Slaughter, B. V.; Peppas, N. A. Polymers for drug delivery systems. *Annu. Rev. Chem. Biomol. Eng.* **2010**, 1, 149.
20. Granados-Hernández, M. V.; Serrano-Bello, J.; Montesinos, J. J.; Alvarez-Gayosso, C.; Medina-Velázquez, L. A.; Alvarez-Fregoso, O.; Alvarez-Perez, M. A. In vitro and in vivo biological characterization of poly (lactic acid) fiber scaffolds synthesized by air jet spinning. *J. Biomed. Mater. Res. B Appl. Biomater.* **2018**, 106(6), 2435–2446.
21. Medeiros, E. S.; Glenn, G. M.; Klamczynski, A. P.; Orts, W. J.; Mattoso, L. H. Solution blow spinning: A new method to produce micro-and nanofibers from polymer solutions. *J. Appl. Polym. Sci***. 2009**, 113(4), 2322–2330.
22. Lou, H.; Han, W.; Wang, X. Numerical study on the solution blowing annular jet and its correlation with fiber morphology. *Ind. Eng. Chem. Res.* **2014**, 53(7), 2830–2838.
23. Bharadwaz, A.; Jayasuriya, A. C. Recent trends in the application of widely used natural and synthetic polymer nanocomposites in bone tissue regeneration. Mater. Sci. Eng. C. **2020**, 110, 110698.
24. Tutak, W.; Sarkar, S.; Lin-Gibson, S.; Farooque, T. M.; Jyotsnendu, G.; Wang, D.; Simon Jr, C. G. The support of bone marrow stromal cell differentiation by airbrushed nanofiber scaffolds. *Biomater.* **2013**, 34(10), 2389–2398.
25. Hoffman, K.; Skrtic, D.; Sun, J.; Tutak, W. Airbrushed composite polymer Zr-ACP nanofiber scaffolds with improved cell penetration for bone tissue regeneration. *Tissue Eng. Part C Methods* **2015**, 21(3), 284–291.
26. Gao, Y.; Yuan, J.; Liu, H.; Yang, Y.; Hou, Y.; Li, S. Tramadol loading, release and iontophoretic characteristics of ion-exchange fiber. *Int. J. Pharm.* **2014**, 465(1-2), 102–111.
27. Kumar, P.; Singh, I. Formulation and characterization of tramadol-loaded IPN microgels of alginate and gelatin: Optimization using response surface methodology. *Acta Pharm.* **2010**, 60(3), 295.
28. Flores-Arriaga, J. C.; Chavarría-Bolaños, D.; Pozos-Guillén, A. D. J.; Escobar-Barrios, V. A.; Cerda-Cristerna, B. I. Synthesis of a PVA drug delivery system for controlled release of a Tramadol-Dexketoprofen combination. *J. Mater. Sci. Mater. Med.* **2021**, 32(5), 1–11.

 doi:10.20944/preprints202505.0085.v1

29. Hatakeyama, T.; Quinn, F. X. Thermal analysis: fundamentals and applications to polymer science. 2º ed.; WILLEY: New Jersey, **1999;** 698
30. Mabrouk, M.; Beherei, H. H.; ElShebiney, S.; Tanaka, M. Newly developed controlled release subcutaneous formulation for tramadol hydrochloride. *Saudi. Pharm. J.* **2018**, 26(4), 585–592.
31. Aamir, M. N.; Ahmad, M. Production and stability evaluation of modified-release microparticles for the delivery of drug combinations. *AAPS PharmSciTech.* **2010**, 11(1), 351–355.
32. Ahad, H. A.; Ishaq, B. M.; Shaik, M.; Bandagisa, F. Designing and characterizing of tramadol hydrochloride transdermal patches prepared with Ficus carica fruit mucilage and povidone. *Pak. J. Pharm. Sci.* **2016**, 29(3), 945–951.
33. Anwar, H.; Ahmad, M.; Minhas, M. U.; Rehmani, S. Alginate-polyvinyl alcohol based interpenetrating polymer network for prolonged drug therapy, optimization and in-vitro characterization. *Carbohydr. Polym.* **2017**, 166, 183–194.
34. Kücük, A.; Kadioğlu, Y. Determination of tramadol hydrochloride in ampoule dosage forms by using UV spectrophotometric and HPLC-DAD methods in methanol and water media. *Farmaco.* **2005**, 60(2), 163–169.
35. Valdivia-Medina, R. Y.; Pedro-Valdés, S.; Laurel-Gómez, M. Agua para uso en laboratorios. *Biol. Sci. Tech. INIMET* **2010**, (1), 3–10.
36. Kareem, M. M.; Hodgkinson, T.; Sanchez, M. S.; Dalby, M. J.; Tanner, K. E. Hybrid core-shell scaffolds for bone tissue engineering. *Biomed. Mater.* **2019**, 14(2), 025008.
37. Chanes-Cuevas, O. A.; Arellano-Sánchez, U.; Alvarez-Gayosso, C. A.; Suaste-Olmos, F.; Villarreal-Ramirez, E.; Alvarez-Fregoso, O.; Alvarez-Perez, M. A. Synthesis of PLA/SBA-15 Composite Scaffolds for Bone Tissue Engineering. *Mater. Res.* **2020**, 23.
38. Osorio-Arciniega, R.; García-Hipólito, M.; Alvarez-Fregoso, O.; Alvarez-Perez, M. A. Composite Fiber Spun Mat Synthesis and In Vitro Biocompatibility for Guide Tissue Engineering. *Molecules* **2021**, 26(24), 7597.
39. Vazquez-Vazquez, F. C.; Chavarria-Bolaños, D.; Ortiz-Magdaleno, M.; Guarino, V.; Alvarez-Perez, M. A. 3D-Printed Tubular Scaffolds Decorated with Air-Jet-Spun Fibers for Bone Tissue Applications. *Bioengineering* **2022**, 9(5), 189.
40. Pereira, M. I. A.; Monteiro, C. A. P.; Oliveira, W. F. D.; Santos, B. S.; Fontes, A.; Cabral Filho, P. E. Resazurin-based assay to evaluate cell viability after quantum dot interaction. QD **2020**, pp. 213–221.
41. Dos Santos, A. C. M.; Akkari, A. C. S.; Ferreira, I. R. S.; Maruyama, C. R.; Pascoli, M.; Guilherme, V. A. ; de Araujo, D. R. Poloxamer-based binary hydrogels for delivering tramadol hydrochloride: sol-gel transition studies, dissolution-release kinetics, in vitro toxicity, and pharmacological evaluation. *Int. J. Nanomedicine* **2015**, 10, 2391.